Langmuir
Article
pubs.acs.org/Langmuir

Solubilization of Poly{1,4-phenylene-[9,9-bis(4-phenoxy-butylsulfonate)] fluorene-2,7-diyl} in Water by Nonionic Amphiphiles

Hugh D. Burrows,*[,†] María J. Tapia,*[,‡] Sofia M. Fonseca,[†] Swapna Pradhan,[§] Ullrich Scherf,[§] Cláudia L. Silva,[†] Alberto A. C. C. Pais,[†] Artur J. M. Valente,[†] Karin Schillén,[∥] Viveka Alfredsson,[∥] Anna M. Carnerup,[∥] Matija Tomšič,[⊥] and Andrej Jamnik[⊥]

[†]*Departamento de Química, and Faculdáde de Farmácia, Universidade de Coimbra, 3004-535 Coimbra, Portugal,* [‡]*Departamento de Química, Universidad de Burgos, Plaza Misael Bañuelos, Burgos 09001, Spain,* [§]*Makromolekulare Chemie, Bergische Universität Wuppertal, D-42097, Germany,* [∥]*Physical Chemistry 1, Center for Chemistry and Chemical Engineering, Lund University, P.O. Box 124, SE-221 00 Lund, Sweden, and* [⊥]*Department of Chemistry and Biochemistry, Faculty of Chemistry and Chemical Technology, University of Ljubljana, Aškerčeva 5, P.O. Box 537, SI-1001 Ljubljana, Slovenia*

Received December 20, 2008. Revised Manuscript Received March 22, 2009

In the presence of the nonionic alkyloxyethylene surfactant *n*-dodecylpentaoxyethylene glycol ether ($C_{12}E_5$), the anionic conjugated polyelectrolyte (CPE) poly{1,4-phenylene-[9,9-bis(4-phenoxy-butylsulfonate)]fluorene-2,7-diyl} (PBS-PFP) dissolves in water, leading to a blue shift in fluorescence and dramatic increases in fluorescence quantum yields above the surfactant critical micelle concentration (cmc). No significant changes were seen with a poly(ethylene oxide) of similar size to the surfactant headgroup, confirming that specific surfactant−polyelectrolyte interactions are important. From UV−visible and fluorescence spectroscopy, dynamic light scattering (DLS), small-angle X-ray scattering (SAXS), cryogenic transmission electron microscopy (cryo-TEM), and electrical conductivity, together with our published NMR and small-angle neutron scattering (SANS) results, we provide a coherent model for this behavior in terms of breakup of PBS-PFP clusters through polymer−surfactant association leading to cylindrical aggregates containing isolated polymer chains. This is supported by molecular dynamics simulations, which indicate stable polymer−surfactant structures and also provide indications of the tendency of $C_{12}E_5$ to break up polymer clusters to form these mixed polymer−surfactant aggregates. Radial electron density profiles of the cylindrical cross section obtained from SAXS results reveal the internal structure of such inhomogeneous species. DLS and cryo-TEM results show that at higher surfactant concentrations the micelles start to grow, possibly partially due to formation of long, threadlike species. Other alkyloxyethylene surfactants, together with poly(propylene glycol) and hydrophobically modified poly(ethylene glycol), also solubilize this polymer in water, and it is suggested that this results from a balance between electrostatic (or ion-dipole), hydrophilic, and hydrophobic interactions. There is a small, but significant, dependence of the emission maximum on the local environment.

1. Introduction

Conjugated polyelectrolytes (CPEs) are advanced materials, which are finding use in chemical and biological sensing,[1−9] two photon singlet oxygen sensitization,[10] electronics or optoelectronics as charge injection or transport layers, and light emitting devices.[11] In addition, polyelectrolytes self-assemble with oppositely charged species, such as surfactants, to build up complex multilayer structures, with various potential materials applications.[12] Early studies by Whitten and co-workers[1] on these polymers as chemical and biological sensors focused on the relatively flexible anionic poly(2,5-methoxy-propyloxysulfonate phenylenevinylene) (MPS-PPV), where it was shown that the fluorescence is dramatically enhanced in the presence of oppositely charged surfactants.[1b] Such surfactant complexation was found to favor electron transfer quenching by neutral molecules, including nitroaromatics,[1c] but it inhibited quenching by cationic quenchers such as methylviologen. Dramatic changes of fluorescence of CPEs have been observed in the presence of various surfactants,[7a,9,13] and Bunz has introduced the concept of surfactochromaticity[7a] to describe this behavior.

Much of the emphasis on CPEs has focused on their potential as extremely efficient fluorescent sensors for biological molecules,

*To whom correspondence should be addressed. (H.D.B.) Departamento de Química, Universidade de Coimbra, 3004-535 Coimbra, Portugal. Telephone: +351 239854482. Fax: +351 239827703. E-mail: burrows@ci.uc.pt. (M.J.T.) Departamento de Química, Universidad de Burgos, Plaza Misael Bañuelos, Burgos 09001, Spain. Telephone: 0034 947 258061. Fax: 0034 947 258831. E-mail: mjtapia@ubu.es.

(1) (a) Chen, L.; McBranch, D. W.; Wang, H.-L.; Helgeson, R.; Wudl, F.; Whitten, D. G. *Proc. Natl. Acad. Sci. U.S.A.* **1999**, *96*, 12287–12292. (b) Chen, L.; Xu, S.; McBranch, D. W.; Whitten, D. *J. Am. Chem. Soc.* **2000**, *122*, 9302–9303. (c) Chen, L.; McBranch, D.; Wang, R.; Whitten, D. *Chem. Phys. Lett.* **2000**, *330*, 27–33. (d) Abe, S.; Chen, L. *J. Polym. Sci., Part B: Polym. Phys.* **2003**, *41*, 1671–1679. (e) Achyuthan, K. E.; Bergstedt, T. S.; Chen, L.; Jones, R. M.; Kumaraswamy, S.; Kushon, S. A.; Ley, K. D.; Lu, L.; McBranch, D.; Mukundan, H.; Rininsland, F.; Shi, X.; Xia, W.; Whitten, D. G. *J. Mater. Chem.* **2005**, *15*, 2648–2656.

(2) (a) Heeger, P. S.; Heeger, A. J. *Proc. Natl. Acad. Sci. U.S.A.* **1999**, *96*, 12219–12221. (b) Wang, D.; Gong, X.; Heeger, P. S.; Rininsland, F.; Bazan, G. C.; Heeger, A. J. *Proc. Natl. Acad. Sci. U.S.A.* **2002**, *99*, 49–53. (c) Fan, C.; Plaxco, K. W.; Heeger, A. J. *J. Am. Chem. Soc.* **2002**, *124*, 5642–5643. (d) Gaylord, B. S.; Heeger, A. J.; Bazan, G. C. *Proc. Natl. Acad. Sci. U.S.A.* **2002**, *99*, 10954–10957. (e) Fan, C.; Plaxco, K. W.; Heeger, A. J. *Trends Biotechnol.* **2005**, *23*, 186–192.

(3) (a) Liu, B.; Gaylord, B. S.; Wang, S.; Bazan, G. C. *J. Am. Chem. Soc.* **2003**, *125*, 6705–6714. (b) Liu, B.; Wang, S.; Bazan, G. C.; Mikhailovsky, A. *J. Am. Chem. Soc.* **2003**, *125*, 13306–13307. (c) Wang, S.; Liu, B.; Gaylord, B. S.; Bazan, G. C. *Adv. Funct. Mater.* **2003**, *13*, 463–467. (d) Wang, S.; Bazan, G. C. *Adv. Mater.* **2003**, *15*, 1425–1428. (e) Dwight, S. J.; Gaylord, B. S.; Hong, J. W.; Bazan, G. C. *J. Am. Chem. Soc.* **2004**, *126*, 16850–16859. (f) Wang, S.; Bazan, G. C. *Chem. Commun.* **2004**, 2508–2509. (g) Mallavia, R.; Martinez-Peréz, D.; Chmelka, B. F.; Bazan, G. C. *Bol. Soc. Esp. Ceram. Vidrio* **2004**, *43*, 327–330. (h) Liu, B.; Bazan, G. C. *J. Am. Chem. Soc.* **2006**, *128*, 1188–1196. (i) Liu, B.; Dan, T. T. T.; Bazan, G. C. *Adv. Funct. Mater.* **2007**, *17*, 2432–2438. (j) Chi, C. Y.; Mikhailovsky, A.; Bazan, G. C. *J. Am. Chem. Soc.* **2007**, *129*, 11134–11145. (k) Sun, C. J.; Gaylord, B. S.; Hong, J. W.; Liu, B.; Bazan, G. C. *Nat. Protoc.* **2007**, *2*, 2148–2151. (l) Hoven, C. V.; Garcia, A.; Bazan, G. C.; Nguyen, T.-Q. *Adv. Mater.* **2008**, *20*, 3793–3810.

such as nucleotides/nucleic acids,[2d,3c,3d,3f,8,9] proteins,[3d,3e] and sugars.[6b] This involves fluorescence quenching or enhancement and follows the ideas of Swager and co-workers[5c,5e] on the amplification of sensor signals of conjugated polymers resulting from their "molecular wire" properties. This can be used for various biosensor strategies,[2d] including transduction of oligonucleotide hybridization.[4a] Fluorene based copolymers are particularly attractive for these[3,4,9,13] because of high fluorescence quantum yields and blue emission.[14] However, CPEs tend to aggregate in water,[1a,3f,6a,7a,11d,13] which reduces both their solubility and fluorescence quantum yields. This is a particularly serious problem with rigid rod polyelectrolytes,[15,16] such as those having poly(*p*-phenylene) units,[15] and the closely related fluorene based polymers.[3,4,9,13] Although aggregation of such systems may be minimized by synthesis of derivatives incorporating appropriate bulky groups,[17] it is frequently more convenient to break up clusters by addition of either an organic cosolvent[3f,6a,11d,13i] or an appropriate surfactant.[7a,9,13a,13c−13g,15f] For example, although stirring the anionic copolymer poly{1,4-phenylene-[9,9-bis(4-phenoxy-butylsulfonate)]fluorene-2,7-diyl} (PBS-PFP) in water leads to formation of a metastable dispersion of polymer clusters,[13c,13i] this can be broken up to give a thermodynamically stable solution by addition of the nonionic surfactant *n*-dodecylpentaoxyethylene glycol ether ($C_{12}E_5$).[13a,13c] Small-angle neutron scattering (SANS) studies,[13d,13g] coupled with NMR measurements,[13c] suggest that this is due to incorporation of the polymer as isolated chains, dissolved at the molecular level, into polymer−surfactant aggregates. Studies of the effect of CPE concentration and addition of NaCl on the clouding behavior indicate that both hydrophobic and electrostatic effects are involved in the CPE−surfactant associative behavior.[18] Results on the behavior of this polymer in solution have been summarized elsewhere.[13i] However, a number of unanswered questions remain, and it is important to try to understand what drives the solubilization of conjugated polyelectrolytes in the presence of nonionic surfactants.

Our earlier studies[13a,13c,13d] on the interactions between $C_{12}E_5$ and PBS-PFP have been extended using dynamic light scattering (DLS), small-angle X-ray scattering (SAXS), cryogenic transmission electron microscopy (cryo-TEM), electrical conductivity, and molecular dynamics simulations. In addition, we have studied the effect of other nonionic surfactants and water-soluble polymers to provide what we believe to be a coherent picture of how these break up PBS-PFP clusters, which may be relevant to the general scenario of the association behavior of CPEs with surfactants.

2. Experimental Section

Materials. The synthesis of poly{1,4-phenylene-[9,9-bis(4-phenoxy-butylsulfonate)]fluorene-2,7-diyl} (PBS-PFP, M_n 6500 g/mol, Figure 1) has been described in detail elsewhere.[13b,13c]

(4) (a) Liu, B.; Bazan, G. C. *Chem. Mater.* **2004**, *16*, 4467–4476. (b) Pinto, M. R.; Schanze, K. S. *Synthesis* **2002**, *9*, 1293–1309.

(5) (a) Swager, T. M. *Acc. Chem. Res.* **1998**, *31*, 201–207. (b) McQuine, D. J.; Pullen, A. E.; Swager, T. M. *Chem. Rev.* **2000**, *100*, 2537–2574. (c) Juan, Z.; Swager, T. M. *Adv. Polym. Sci.* **2005**, *177*, 151–179. (d) Joly, G. D.; Geiger, L.; Kooi, S. E.; Swager, T. M. *Macromolecules* **2006**, *39*, 7175–7177. (e) Thomas, S. W.; Joly, G. D.; Swager, T. M. *Chem. Rev.* **2007**, *107*, 1339–1386. (f) Satrijo, A.; Swager, T. M. *J. Am. Chem. Soc.* **2007**, *129*, 16020–16028.

(6) (a) Tan, C.; Pinto, M. R.; Schanze, K. S. *Chem. Commun.* **2002**, 446–447. (b) DiCesare, N.; Pinto, M. R.; Schanze, K. S.; Lakowicz, J. R. *Langmuir* **2002**, *18*, 7785–7787. (c) Tan, C.; Atas, E.; Müller, J. G.; Pinto, M. R.; Kleinman, V. D.; Schanze, K. S. *J. Am. Chem. Soc.* **2004**, *126*, 13685–13694. (d) Haskins-Glusac, K.; Pinto, M. R.; Tan, C.; Schanze, K. S. *J. Am. Chem. Soc.* **2004**, *126*, 14964–14971. (e) Tan, C. Y.; Pinto, M. R.; Kose, M. E.; Ghiviriga, I.; Schanze, K. S. *Adv. Mater.* **2004**, *16*, 1208–1212. (f) Pinto, M. R.; Schanze, K. S. *Proc. Natl. Acad. Sci. U.S.A.* **2004**, *101*, 7505–7510. (g) Müller, J. G.; Atas, E.; Tan, C.; Schanze, K. S.; Kleiman, V. D. *J. Am. Chem. Soc.* **2006**, *128*, 4007–4016. (h) Liu, Y.; Ogawa, K.; Schanze, K. S. *Anal. Chem.* **2008**, *80*, 150–158. (i) Zhai, X. Y.; Jiang, H.; Schanze, K. S. *Macromolecules* **2008**, *41*, 3422–3428.

(7) (a) Lavigne, J. J.; Broughton, D. L.; Wilson, J. N.; Erdogan, B.; Bunz, U. H. F. *Macromolecules* **2003**, *36*, 7409–7412. (b) Kim, I.-B.; Dunkhorst, A.; Gilbert, J.; Bunz, U. H. F. *Macromolecules* **2005**, *38*, 4560–4562. (c) Kim, I.-B.; Phillips, R.; Bunz, U. H. F. *Macromolecules* **2007**, *40*, 814–817. (d) McRae, R. L.; Phillips, R. L.; Kim, I. B.; Bunz, U. H. F.; Fahmi, C. J. *J. Am. Chem. Soc.* **2008**, *130*, 7851–7853.

(8) Taira, S.; Yokoyama, K. *Biotechnol. Bioeng.* **2004**, *88*, 35–41.

(9) (a) Al Attar, H. A.; Monkman, A. P. *J. Phys. Chem. B* **2007**, *111*, 12418–12426. (b) Al Attar, H. A.; Monkman, A. P. *Adv. Funct. Mater.* **2008**, *18*, 1–12. (c) Nayak, R. R.; Nag, O. K.; Kang, M.; Jin, Y.; Suh, H.; Lee, K.; Woo, H. Y. *Macromol. Rapid Commun.*, published online Mar 16, http://dx.doi.org/.

(10) Nielsen, C. B.; Johnsen, M.; Arnbjerg, J.; Pittelkow, M.; McIlroy, S. P.; Ogilby, P. R.; Jørgensen, M. *J. Org. Chem.* **2005**, *70*, 7065–7079.

(11) (a) Dang, T. D.; Bai, S. J.; Heberer, D. P.; Arnold, F. E.; Spry, R. J. *J. Polym. Sci., Part B: Polym. Phys.* **1993**, *31*, 1941–1950. (b) Xia, C.; Locklin, J.; Youk, J. H.; Fulghum, T.; Advincula, R. C. *Langmuir* **2002**, *18*, 955–957. (c) Huang, F.; Wu, H.; Wang, D.; Yang, W.; Cao, Y. *Chem. Mater.* **2004**, *16*, 708–716. (d) Huang, F.; Hou, L.; Wu, H.; Wang, X.; Shen, H.; Cao, W.; Yang, W.; Cao, Y. *J. Am. Chem. Soc.* **2004**, *126*, 9845–9853. (e) Ma, W.; Iyer, P. K.; Gong, X.; Liu, B.; Moses, D.; Bazan, G. C.; Heeger, A. J. *Adv. Mater.* **2005**, *17*, 274–277. (f) Wilson, J. S.; Frampton, M. J.; Michels, J. J.; Sardone, L.; Marletta, G.; Friend, R. H.; Samori, P.; Anderson, H. L.; Cacialli, F. *Adv. Mater.* **2005**, *17*, 2659–2663. (g) Mwaura, J. K.; Pinto, M. R.; Witker, D.; Ananthakrishnan, N.; Schanze, K. S.; Reynolds, J. R. *Langmuir* **2005**, *21*, 10119–10126. (h) Liu, B.; Bazan, G. C. *Macromol. Rapid Commun.* **2007**, *28*, 1804–1808. (i) Yang, R. D.; Xu, H.; Dang, X. D.; Nguyen, T. Q.; Cao, Y.; Bazan, G. C. *J. Am. Chem. Soc.* **2008**, *130*, 3282–3283.

(12) (a) Decher, G. *Science* **1997**, *277*, 1232–1237. (b) Baur, J. W.; Kim, S.; Balanda, P. B.; Reynolds, J. R.; Rubner, M. F. *Adv. Mater.* **1998**, *10*, 1452–1455. (c) Baur, J. W.; Rubner, M. F.; Reynolds, J. R.; Kim, S. *Langmuir* **1999**, *15*, 6460–6469. (d) Fendler, J. H. *Chem. Mater.* **2001**, *13*, 3196–3210. (e) Kim, D. H.; Hernandez-Lopez, J. L.; Liu, G.; Mihov, G.; Zhi, L.; Bauer, R. E.; Grebel-Köhler, D.; Klapper, M.; Weil, T.; Müllen, K.; Mittler, S.; Knoll, W. *Macromol. Chem. Phys.* **2005**, *206*, 52–58.

(13) (a) Burrows, H. D.; Lobo, V. M. M.; Pina, J.; Ramos, M. L.; Seixas de Melo, J.; Valente, A. J. M.; Tapia, M. J.; Pradhan, S.; Scherf, U. *Macromolecules* **2004**, *37*, 7425–7427. (b) Tapia, M. J.; Burrows, H. D; Valente, A. J. M.; Pradhan, S.; Scherf, U.; Lobo, V. M. M.; Pina, J.; Seixas de Melo, J. *J. Phys. Chem. B* **2005**, *109*, 19108–19115. (c) Burrows, H. D.; Lobo, V. M. M.; Pina, J.; Ramos, M. L.; Seixas de Melo, J.; Valente, A. J. M.; Tapia, M. J.; Pradhan, S.; Scherf, U.; Hintschich, S. I.; Rothe, C.; Monkman, A. P. *Colloids Surf., A* **2005**, *270−271*, 61–66. (d) Knaapila, M.; Almásy, L.; Garamus, V. M.; Pradhan, S.; Pearson, C.; Petty, M. C.; Scherf, U.; Burrows, H. D.; Monkman, A. P. *J. Phys. Chem. B* **2006**, *110*, 10248–10257. (e) Tapia, M. J.; Burrows, H. D.; Knaapila, M.; Monkman, A. P.; Arroyo, A.; Pradhan, S.; Scherf, U.; Pinazo, A.; Pérez, L.; Morán, C. *Langmuir* **2006**, *22*, 10170–10174. (f) Burrows, H. D.; Tapia, M. J.; Silva, C. L.; Pais, A. A. C. C.; Fonseca, S. M.; Pina, J.; Seixas de Melo, J.; Wang, Y.; Marques, E. F.; Knaapila, M.; Monkman, A. P.; Garamus, V. M.; Pradhan, S.; Scherf, U. *J. Phys. Chem. B* **2007**, *111*, 4401–4410. (g) Burrows, H. D.; Knaapila, M.; Monkman, A. P.; Tapia, M. J.; Fonseca, S. M.; Ramos, M. L.; Pyckhout-Hintzen, W.; Pradhan, S.; Scherf, U. *J. Phys.: Condens. Matter* **2008**, *20*, 104210. (h) Monteserín, M.; Burrows, H. D.; Valente, A. J. M.; Lobo, V. M. M.; Mallavia, R.; Tapia, M. J.; García-Zubiri, I. X.; Di Paolo, R. E.; Maçanita, A. L. *J. Phys. Chem. B* **2007**, *111*, 13560–13569. (i) Burrows, H. D.; Fonseca, S. M.; Silva, C. L.; Pais, A. A. C. C.; Tapia, M. J.; Pradhan, S.; Scherf, U. *Phys. Chem. Chem. Phys.* **2008**, *10*, 4420–4428. (j) Burrows, H. D.; Tapia, M. J.; Fonseca, S. M.; Valente, A. J. M.; Lobo, V. M. M.; Justino, L. L. G.; Qiu, S.; Pradhan, S.; Scherf, U.; Chattopadhyay, N.; Knaapila, M.; Garamus, V. M. *ACS Appl. Mater. Interfaces*, published online Mar 20, http://dx.doi.org/.

(14) (a) Ohmori, Y.; Uchida, M.; Muro, K.; Yoshino, K. *Jpn. J. Appl. Phys., Part 2* **1991**, *30*, L1941–L1943. (b) Grice, A. W.; Bradley, D. D. C.; Bernius, M. T.; Inbasekaran, M.; Wu, W. E.; Woo, E. P. *Appl. Phys. Lett.* **1998**, *73*, 629–631. (c) Leclerc, M. *J. Polym. Sci., Part A: Polym. Chem.* **2001**, *39*, 2867–2873. (d) Scherf, U.; List, E. J. W. *Adv. Mater.* **2002**, *14*, 477–487. (e) Knaapila, M.; Winokur, M. J. *Adv. Polym. Sci.* **2008**, *212*, 227–272. (f) Monkman, A.; Rothe, C.; King, S.; Dias, F. *Adv. Polym. Sci.* **2008**, *212*, 187–225.

(15) (a) Rulkens, R.; Wegner, G.; Thurn-Albrecht, T. *Langmuir* **1999**, *15*, 4022–4025. (b) Bockstaller, M.; Köhler, W.; Wegner, G.; Vlassopoulos, D.; Fytas, G. *Macromolecules* **2000**, *33*, 3951–3953. (c) Bockstaller, M.; Köhler, W.; Wegner, G.; Fytas, G. *Macromolecules* **2001**, *34*, 6353–6358. (d) Bockstaller, M.; Köhler, W.; Wegner, G.; Vlassopoulos, D.; Fytas, G. *Macromolecules* **2001**, *34*, 6359–6366. (e) Zaroslov, Yu. D.; Gordeliy, V. I.; Kiklin, A. I.; Islamov, A. H.; Philippova, O. E.; Khokhlov, A. R.; Wegner, G. *Macromolecules* **2002**, *35*, 4466–4471. (f) Fütterer, T.; Hellweg, T.; Findenegg, G. H.; Frahn, J.; Schlüter, A. D. *Macromolecules* **2005**, *38*, 7451–7455.

(16) (a) Ballauff, M. *Angew. Chem., Int. Ed.* **1989**, *28*, 253–267. (b) Wegner, G. *Macromol. Chem. Phys.* **2003**, *204*, 347–357. (c) Stepanyan, R.; Subbotin, A.; Knaapila, M.; Ikkala, O.; Ten Brinke, G. *Macromolecules* **2003**, *36*, 3758–3763. (d) Limbach, H. J.; Holm, C.; Kremer, K. *Macromol. Chem. Phys.* **2005**, *206*, 77–82. (e) Knaapila, M.; Stepanyan, R.; Lyons, B. P.; Torkeli, M.; Monkman, A. P. *Adv. Funct. Mater.* **2006**, *16*, 599–609.

(17) (a) Khan, A.; Müller, S.; Hecht, S. *Chem. Commun.* **2005**, 584–586. (b) Lee, K.; Cho, J. C.; DeHeck, J.; Kim, J. *Chem. Commun.* **2006**, 1983–1985.

(18) Fonseca, S. M.; Eusébio, M. E.; Castro, R.; Burrows, H. D.; Tapia, M. J.; Olsson, U. *J. Colloid Interface Sci.* **2007**, *315*, 805–809.

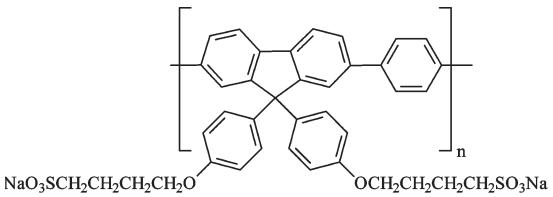

PBS-PFP

$CH_3 - (CH_2)_x (OCH_2CH_2)_y OH$

	x	y
$C_{10}E_3$	9	3
$C_{12}E_4$	11	4
$C_{12}E_5$	11	5

Triton X-100 (m ≈ 9 – 10)

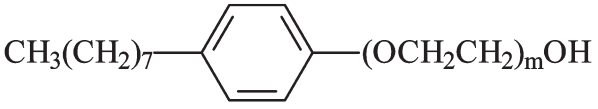

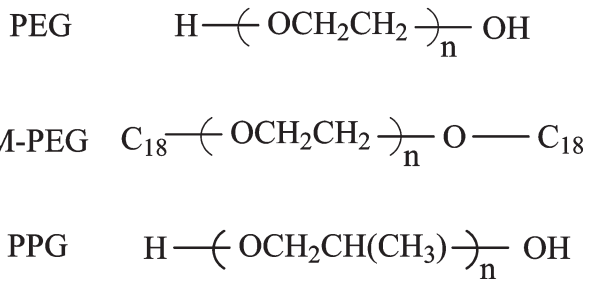

Figure 1. Structures of polymers and surfactants used. For HM-PEG, C_{18} corresponds to the *n*-octadecyl group $C_{18}H_{37}$.

The structures of the nonionic surfactants and polymers used in this study are given in Figure 1. Pure *n*-decyltrioxyethylene glycol ether $C_{10}E_3$, *n*-dodecyltetraoxyethylene glycol ether $C_{12}E_4$, and *n*-dodecylpentaoxyethylene glycol ether $C_{12}E_5$ were gifts from Professor Ulf Olsson (Lund University), had greater than 99% purity, and were used without further treatment. Experiments were also carried out with commercial $C_{12}E_5$ (Fluka) and gave similar results. However, although the results were qualitatively similar with commercial $C_{12}E_4$ (Sigma), differences were observed at the quantitative level, as seen in the cloud point behavior,[18] and are probably due to the presence of other alkyloxyethylene surfactants. Triton X-100, poly(ethylene glycol) (PEG 200, 10 000 molecular weight ($\overline{M}_n$)), and poly(propylene glycol) (PPG) were acquired from Aldrich and used as received. Hydrophobically modified poly(ethylene glycol) (HM-PEG) was from Akzo Nobel Surface Chemistry and was used without further purification. This polymer is a hydrophobically end-capped copolymer, having octadecyl (C_{18}) chains at both ends and a polar midblock composed of ca. 300 oxyethylene units. The average molecular weight ($\overline{M}_n$) is approximately 14 000 g/mol. Such types of polymers show a low polydispersity (around 1.1).

All experiments were carried out in solutions in Milli-Q Millipore water. Solutions of PBS-PFP with various concentrations up to 6.8×10^{-3} g/L (corresponding to 9.18×10^{-6} (moles repeat unit)/L) were freshly prepared and were stirred overnight before use. For the photophysical experiments with nonionic surfactants, freshly prepared aqueous stock solutions of surfactant were used with concentrations between 10^{-2} and 10^{-1} M. Where appropriate, these were diluted to give lower concentration stock solutions, enabling studies over the whole surfactant concentration range used in this study (3×10^{-8} to around 5×10^{-3} M). For dynamic light scattering studies, solutions were prepared with 8×10^{-2} g/L PBS-PFP (corresponding to 1.1×10^{-4} (moles repeat unit)/L) and $C_{12}E_5$ concentrations varying from 3.12×10^{-5} to 1.10×10^{-3} M. Similarly, for conductivity experiments, a polymer concentration of 1.2×10^{-4} M (in terms of repeat units) and the surfactant concentration were varied in the same range. The samples for SAXS measurements contained 12.7×10^{-3} M $C_{12}E_5$ and 0.39 g/L PBS-PFP (corresponding to 5.2×10^{-4} (moles repeat unit)/L).

Cryo-TEM was performed on both a $C_{12}E_5$ solution alone and one mixed with PBS-PFP. A solution of 2.15×10^{-3} (moles repeat unit)/L PBS-PFP was prepared and stirred overnight before being mixed with $C_{12}E_5$, giving a final concentration of 19×10^{-3} M $C_{12}E_5$ ($C_{12}E_5$/PBS-PFP (repeat unit) molar ratio of 8.8). In addition, a solution of 19×10^{-3} M $C_{12}E_5$ alone was also prepared, and both solutions were left stirring for 1 h before samples were prepared for cryo-TEM.

Instrumentation and Methods. Absorption and luminescence spectra were recorded on Shimadzu UV-2100 and Jobin-Ivon SPEX Fluorolog 3-22 spectrometers, respectively. Fluorescence spectra were registered with excitation at 381 nm and were corrected for the wavelength response of the system. When not being used for measurements, all samples were kept in the absence of light. Fluorescence quantum yields were measured using quinine sulfate in 0.5 M sulfuric acid as standard.[19]

For the electrical conductivity measurements, electrical resistances were measured on solutions with a Wayne-Kerr model 4265 Automatic LCR meter at 1 kHz and a Shedlovsky-type conductance cell.[13b,20] The cell constant (approximately 0.1012 cm^{-1}) was determined to ±0.02% from measurements with KCl (reagent grade, recrystallized and dried using the procedure and data from Barthel et al.[21]). Measurements were made at 25.00 ± 0.01 °C in a Grant thermostat bath.

The setup for the dynamic light scattering (DLS) and static light scattering (SLS) measurements employed an ALV/DLS/SLS-5000F, CGF-8F based compact goniometer system from ALV-GmbH, Langen, Germany. The light source was a Nd:YAG solid-state Compass-DPSS laser (Coherent Inc., Santa Clara, CA), which operates at 532 nm with a fixed output power, which is varied externally by an attenuator. In the DLS measurements, which were performed at different angles between 40 and 120°, the time correlation function (pseudocross or auto) of the scattered intensity was obtained by using two multiple tau digital correlators with 320 spaced channels. The mixed polymer−surfactant solutions were investigated either unfiltered or filtered through sterile, hydrophilic Minisart filters with a 0.45 (or larger) μm pore diameter (Sartorius, Germany). However, the water used in the preparation of the solutions was pre-filtered and purified by a Milli-Q system from Millipore Corporation, Bedford, MA, which

(19) Miller, J. N., Ed. *Standards in Fluorescence Spectrometry*; Chapman and Hall: London, **1981.**

(20) Ribeiro, A. C. F.; Valente, A. J. M.; Azevedo, E. F. G.; Amado, A. M.; Amorim da Costa, A. M.; Ramos, M. L.; Burrows, H. D. *J. Mol. Struct.* **2004**, *703*, 93–101.

(21) Barthel, J.; Feuerlein, F.; Neuder, R.; Wachter, R. *J. Sol. Chem.* **1980**, *9*, 209–219.

includes a sterile filter with 0.22 μm pore diameter. In the present study, the temperature was set to 25.00 °C and controlled to within ±0.01 °C. Measurements were also performed at room temperature (≈23 °C). The absolute light scattering intensity was obtained as an additional output from the DLS measurements. Cylindrical light scattering cells of borosilicate glass, cleaned with Hellmanex cleaning solution, were used. The DLS analyses were made using the method of nonregular inverse Laplace transformation of the measured intensity correlation functions using the algorithm REPES,[22,23] from which the distribution of relaxation times is obtained. The distributions are given in the form $\tau A(\tau)$ versus $\log_{10}(\tau/\mu s)$, where τ is the relaxation time providing equal area representation. Diffusion coefficients are calculated from the distribution moments as:

$$D = (\Gamma/q^2)_{q\to 0} \quad (1)$$

where Γ is the relaxation rate ($=1/\tau$) and q is the magnitude of the scattering vector ($q = (4\pi n/\lambda)\sin\theta/2$, in which n is the refractive index of the medium (here water), λ is the laser wavelength, and θ is the scattering angle). A detailed description of the DLS/SLS equipment and the data analysis is given elsewhere.[24,25]

Small-Angle X-ray scattering spectra were measured with a so-called "Kratky compact camera"[26] attached to an X-ray generator operating at 35 kV and 35 mA on a sealed X-ray tube (copper anode, $\lambda = 0.154$ nm). The samples were measured in a standard quartz capillary with an outer diameter of 1 mm and wall thickness of 10 μm. SAXS intensities were detected with the position sensitive detector PSD ASA in the regime $0.05 < q < 7$ nm^{-1} where we here define $q = (4\pi/\lambda)\sin(\theta/2)$. Due to the low excess scattering of the two samples, the measuring times were up to 72 h in order to ensure reasonable statistics. Scattering data were first averaged and corrected for the solvent scattering and finally put on absolute scale using water as a secondary standard.[27] The SAXS data obtained in this way were still experimentally smeared because of the finite dimensions of the primary beam.[28] For further evaluation, the indirect Fourier transformation software package IFT[29] was used. This method is completely model-free and can only be successfully applied for the systems where interparticle interactions can be neglected. The latter was a good approximation in our case due to the very low concentrations of the structuring material in the studied samples. According to our previous studies using SANS,[13d,13g] these samples were suggested to contain wormlike micelles; therefore, IFT was used in a mode for evaluating cylindrical particles. Resulting pair−distance distribution function of the cross section, $p_c(r)$, served as a tool for the determination of the scattering particles' cross-sectional geometry. In this approximation, the scattering intensity from one scattering particle, $I_1(q)$, is written as the Hankel transformation of the $p_c(r)$ function:[28]

$$I_1(q) = 2\pi^2 L \int_0^\infty p_c(r)\,\frac{J_0(qr)}{q}\,dr \quad (2)$$

where $J_0(qr)$ is the zero-order Bessel function, L is the length of the cylinder, and r is the distance between two scattering centers within the particle. A constant electron density is assumed along the cylinder axis. In such a case, the $p_c(r)$ function directly represents a histogram of distances inside the scattering particle's cross section.[30,31] At distances r larger than the cross-sectional diameter, the $p_c(r)$ function adopts the value of zero. This provides a useful tool for the determination of the cross-sectional diameter. Furthermore, the convolution square root can be calculated from the $p_c(r)$ function, yielding the radial electron density profile of the cross section $\Delta\rho_c(r)$, which reveals the internal structure of the scattering particle.[31−34] In the case of an axially homogeneous cylinder, the $p_c(r)$ function is identical to:[26]

$$p_c(r) = r\Delta\tilde{\rho}_c{}^2(r) \quad (3)$$

where $\Delta\tilde{\rho}_c^2$ is the spatially averaged autocorrelation function (convolution square) of the electron density fluctuations in the cross section given by the general expression:[31]

$$\Delta\tilde{\rho}_c{}^2(r) = \langle\Delta\tilde{\rho}_c{}^2(\mathbf{r})\rangle = \left\langle \int_{-\infty}^{\infty} \Delta\rho_c(\mathbf{r}_1)\,\Delta\rho_c(\mathbf{r}_1-\mathbf{r})\,d\mathbf{r}_1 \right\rangle \quad (4)$$

with $\Delta\rho_c(r)$ representing the local scattering contrast.

For the cryo-TEM analysis, samples were prepared using a controlled environment vitrification system (CEVS),[35] where the relative humidity was kept close to saturation at around 28 °C. A 5 μL drop was placed on a lacy carbon-coated copper grid, and the excess fluid was gently blotted away, leaving a thin film of aqueous sample covering the grid. The grid was then plunged into liquid ethane at −180 °C to allow rapid vitrification of the specimen (avoiding crystallization of water). All prepared grids were stored in liquid nitrogen until being transferred to the electron microscope. Images were digitally recorded at around −183 °C using a Philips CM120 Bio TWIN electron microscope, operated at 120 kV and equipped with a Gatan MSC791 cooled-CCD camera system. To minimize beam damage, all samples were imaged under minimal electron dose conditions.

Simulations were performed using the GROMACS software package with the standard GROMACS force field,[36,37] which is a modified version of the GROMOS87 force field.[38] Topology files were generated from initial structures, in Cartesian coordinates, resorting to the PRODRG server.[39] The molecules are added to a box and solvated with single point charge (SPC) model water,[40] with the structure constrained by the SETTLE algorithm.[41] The SPC model for water considers three interaction sites centered on the atomic nuclei; the intramolecular degrees of freedom are frozen, while the intermolecular interactions are described by a conjunction of Lennard−Jones 12-6 potential and Coulombic potentials between sites with fixed point charges.

We note that this simple model has been considered to accurately reproduce many properties of bulk water, especially under normal conditions: 300 K and 1 atm.[42] It was also shown to be

(22) Jakěs, J. *Collect. Czech. Chem. Commun.* **1995**, *60*, 1781–1797.
(23) Štěpánek, P. In *Dynamic Light Scattering: The Method and Some Applications*; Brown, W., Ed.; Oxford University Press: Oxford, **1993; p 177.**
(24) (a) Jansson, J.; Schillén, K.; Olofsson, G.; Cardoso da Silva, R.; Loh, W. *J. Phys. Chem. B* **2004**, *108*, 82–92. (b) Löf, D.; Niemiec, A.; Schillén, K.; Loh, W.; Olofsson, G. *J. Phys. Chem. B* **2007**, *111*, 5911–5920.
(25) Schillén, K.; Jansson, J.; Löf, D.; Costa, T. *J. Phys. Chem. B* **2008**, *112*, 5551–5562.
(26) Kratky, O.; Stabinger, H. *Colloid Polym. Sci.* **1984**, *262*, 345–360.
(27) Orthaber, D.; Bergmann, A.; Glatter, O. *J. Appl. Crystallogr.* **2000**, *33*, 218–225.
(28) Glatter, O. In *Small Angle X-Ray Scattering*; Glatter, O., Kratky, O., Eds.; Academic Press Inc. London Ltd.: London, **1983; pp 119−165.**
(29) Glatter, O. *J. Appl. Crystallogr.* **1977**, *10*, 415–421.
(30) Glatter,O. In *Small Angle X-Ray Scattering*; Glatter, O, Kratky, O., Eds.; Academic Press Inc. London Ltd.: London, **1983; pp 167−196.**
(31) Glatter, O. In *Neutron, X-rays and Light: Scattering Methods Applied to Soft Condensed Matter*; Lindner, P., Zemb, T., Eds.; Elsevier: North Holland, Amsterdam, **2002.**
(32) Glatter, O. *J. Appl. Crystallogr.* **1981**, *14*, 101–108.
(33) Glatter, O.; Hainisch, B. *J. Appl. Crystallogr.* **1984**, *17*, 435–441.
(34) Mittelbach, R.; Glatter, O. *J. Appl. Crystallogr.* **1998**, *31*, 600–608.
(35) Bellare, J. R.; Davis, H. T.; Scriven, L. E.; Talmon, Y. *J. Electron Microsc. Tech.* **1988**, *10*, 87–111.
(36) Berendsen, H. J. C.; van der Spoel, D.; van Drunen, R. *Comput. Phys. Commun.* **1995**, *91*, 43–56.
(37) Lindhal, E.; Hess, B.; van der Spoel, D. *J. Mol. Model.* **2001**, *7*, 306–317.
(38) van Gunsteren, W. F.; Berendsen, H. J. C. *Gromos-87 manual*; Biomos BV, Nijenborgh 4: 9747 AG Groningen, The Netherlands, **1987.**
(39) van Aalten, D. M. F.; Bywater, R.; Findlay, J. B. C.; Hendlich, M.; Hooft, R. W. W.; Vriend, G. *J. Comput.-Aided Mol. Des.* **1996**, *10*, 255–263.
(40) Berendsen, H. J. C.; Postma, J. P. M.; van Gunsteren, W. F.; Hermans, J. Interaction models for water in relation to protein hydration. In *Intermolecular Forces*; Pullman, B., Ed.; Reidel: Dordrecht, **1981; pp 331−342.**
(41) Miyamoto, S.; Kollman, P. A. *J. Comput. Chem.* **1992**, *13*, 952–962.
(42) Wu, Y.; Tepper, H. L.; Voth, G. A. *J. Chem. Phys.* **2006**, *124*, 024503.

superior to other water models[43,44] and has been recommended for modeling aqueous solutions of biomolecules.[45] It has also been previously employed in systems comprising interactions similar to those of the present work.[13i,46]

Previous to each molecular dynamics (MD) simulation, an energy minimization was performed. This was followed by a MD equilibration run under position restraints for 5 ns. An unrestrained MD run was then carried out for 2 ns, as a further equilibration simulation. Finally, a MD trajectory was generated with a step time of 2 fs for each model system (see below). All simulations were performed with periodic boundary conditions, using the Berendsen coupling algorithm (P = 1 bar, τ_p = 0.5 ps; T = 300 K, τ_t = 0.1 ps)[47] for ensuring NPT conditions (constant number of particles N, pressure P, temperature T). The particle mesh Ewald method[48] was used for computation of long-range electrostatic forces.

3. Results and Discussion

In subsections A and B, we will present the results of the experimental and molecular dynamics simulation studies of the interaction between PBS-PFP and $C_{12}E_5$ in aqueous solution, and in subsection C we extend the experimental study to the interaction of PBS-PFP with other alkyloxyethylene surfactants together with water-soluble poly(ethylene glycol) and poly (propylene glycol) polymers to gain insight into the factors involved in the breaking up of PBS-PFP clusters through their interaction with neutral amphiphilic compounds.

A. Experimental Studies on Aqueous PBS-PFP/$C_{12}E_5$ Solutions. We have previously shown that addition of the nonionic surfactant $C_{12}E_5$ to aqueous dispersions of PBS-PFP leads to a blue shift in absorption and emission maxima and to a marked increase in fluorescence quantum yield.[13a,13c] Typical absorption and fluorescence spectra in water in the absence and presence of surfactant are given in the Supporting Information (Figure S1). Fluorescence spectra show some vibronic structure, both in the absence and presence of surfactant. The fluorescence quantum yield value observed here with $C_{12}E_5$ is slightly higher than that which we previously reported (0.6).[13a] However, the maximum surfactant concentration used in this case is also higher. This enhancement of fluorescence intensity with $C_{12}E_5$ is accompanied by an increase in the fluorescence lifetime (from ca. 250 to 500 ps).[13a] In contrast, as shown previously,[13a] and as will be discussed in part C, with a polymer of similar size (PEG, 200 molecular weight ($\overline{M}_n$)) to the ethylene oxide headgroup of $C_{12}E_5$, only slight changes in fluorescence intensity are observed in the presence of poly(ethylene oxide), with no change in band shape or maxima, showing that the simultaneous presence of both the alkyl chain and ethylene oxide headgroup are important for the observed behavior.

Evidence has been presented elsewhere that the polymer is present in water as clusters.[13i] Although, as we will discuss in subsection CC, this is not the only explanation for the observed spectral changes, we believe that the surfactant is breaking up these clusters to form new surfactant−polymer aggregates. However, fluorescence spectra alone are unable to unambiguously confirm this, so to gain further insight into the process and the nature of these species dynamic light scattering measurements were performed at various angles on PBS-PFP/$C_{12}E_5$ solutions with $C_{12}E_5$/PBP-PFP molar ratios ranging from 0.3 to 10.5 and polymer concentrations of 1.1×10^{-4} (moles repeat unit)/L. These are similar molar ratios to those used in our previous SANS study on this system.[13d] The solutions were first measured unfiltered and subsequently were passed through filters with 0.45 μm pore size. (Filtering through 0.2 μm pore sized filters was also tested.) A difference between unfiltered and filtered solutions was observed at high molar ratios, suggesting the formation of large aggregates with sizes of several hundred nanometers. In this case, we, therefore, present the data of the unfiltered solutions. In Figure 2, we present a selection of relaxation time distributions obtained from inverse Laplace transformation of the intensity correlation functions for various $C_{12}E_5$/PBS-PFP molar ratios.

At low molar ratios (MR < 0.6, which corresponds to concentrations below the critical micelle concentration (cmc) of $C_{12}E_5$, regime 1), the distributions are characterized by a single broad mode (Figure 2a), which is diffusive. This was established from the linear q^2 dependence of the corresponding mean relaxation rate Γ (data not shown). We thus attribute this mode to the translational diffusion process of polymer clusters containing several chains, together with associated $C_{12}E_5$ monomers.

At intermediate molar ratios 1.1 ≤ MR ≤ 3.5 (regime 2, Figure 3a), which corresponds to $C_{12}E_5$ concentrations around and above the cmc, the distributions become bimodal, with a low-amplitude peak appearing at shorter relaxation times in addition to the slower translational mode. At these molar ratios, based on previous results on the system from fluorescence, NMR, electrical conductivity, and SANS,[13a,13c,13d] the polymer clusters are broken up due to the interaction with the $C_{12}E_5$ molecules and polymer−surfactant complexes are formed that consist of one polymer chain and several $C_{12}E_5$ unimers. From previous neutron scattering studies on these and similar systems,[13d,13g] NMR self-diffusion studies on the related cationic poly-(9,9-bis(6′-*N*,*N*,*N*-trimethylammonium)hexyl)-fluorene phenylene) bromide (unpublished results), together with molecular dynamics calculations presented below, we believe the complex is cylindrical in shape. With this in mind, the fast mode observed may, therefore, originate from the mode coupling between the translational and rotational diffusion of the complex. We were unable to further investigate the angular dependence of this mode due to the fact that the polydispersity of the polymer−surfactant complexes was too large, thus affecting the accuracy of the data points. Furthermore, the broadening of the slow mode increased from molar ratio 0.6 to 3.5, which indicates a growth into more polydisperse complexes.

At high molar ratios, MR > 5 (regime 3, Figure 2b), the distributions are clearly bimodal and the fast mode grows in amplitude at the expense of the slow mode. In this regime, the complexes grow into larger elongated structures, possibly consisting of several polymer−surfactant complexes attached to each other in a head-to-tail fashion. The origin of the fast mode may then reflect the mode coupling between translational and internal motion of these structures. The results presented in Figure 2b are for the unfiltered solutions. For freshly filtered solutions (0.45 μm) with molar ratios 5.8 and 10.5, DLS measurements could not be performed at 90° due to too low scattering intensity, which indicates a material loss in the filtration process due to the formation and separation of large supramolecular structures.

The apparent collective (or mutual) diffusion coefficients of the translational motion of the complexes were obtained from the slope of the linear q^2 dependence of the relaxation rate of the translational mode ($D = \Gamma/q^2$, eq 1). There was a slight deviation in the linearity, which is in turn reflected in the size polydispersity of the complexes (data not shown). The D values are presented as

(43) vanderSpoel, D.; Berendsen, H. J. C. *Biophys. J.* **1997**, *72*, 2032–3041.
(44) Tieleman, D. P.; Berendsen, H. J. C. *J. Chem. Phys.* **1996**, *105*, 4871–4880.
(45) Zielkiewicz, J. *J. Chem. Phys.* **2005**, *123*, 104501–104506.
(46) Friedman, R. E.; Nachlief, E.; Gutman, M. *Biophys. J.* **2005**, *89*, 768–781.
(47) Berendsen, H. J. C.; Postma, J. P. M.; DiNola, A.; Haak, J. R. *J. Chem. Phys.* **1984**, *81*, 3684–3690.
(48) Darden, T.; York, D.; Pedersen, L. *J. Chem. Phys.* **1993**, *98*, 10089–10092.

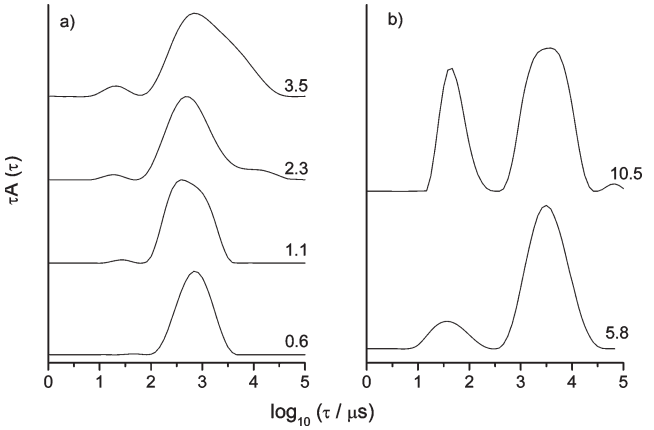

Figure 2. Relaxation time distributions obtained from inverse Laplace transformation of the corresponding intensity correlation functions for different $C_{12}E_5$/PBS-PFP molar ratios at 298 K: (a) data collected at $\theta = 120°$ and (b) data collected at $\theta = 90°$. An estimate of the length of suggested rodlike aggregates is given in the text.

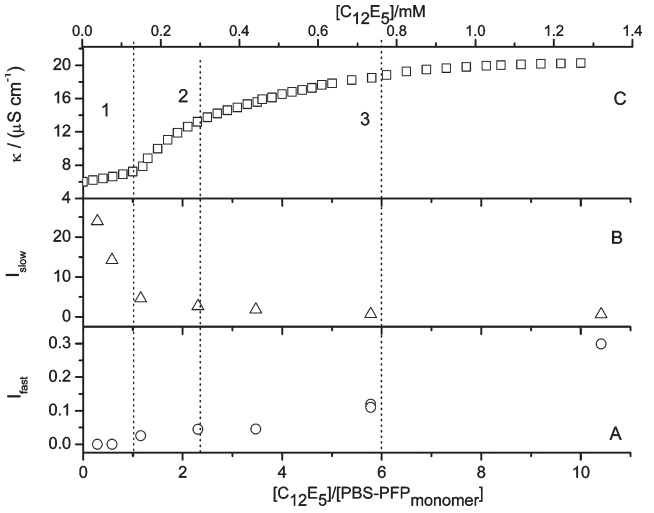

Figure 3. Comparison between (a) fast and (b) slow static light scattering intensities (I_{fast} and I_{slow}) at 90°, obtained from the amplitudes of the slow and fast mode, normalized to the incoming laser intensity, and (c) specific conductivity as a function of both $C_{12}E_5$/PBS-PFP molar ratio and $C_{12}E_5$ concentration. Regions 1, 2, and 3 correspond to the three surfactant/CPE phase regimes presented in our previous SANS study.[13d]

a function of the $C_{12}E_5$/PBS-PFP molar ratio in the Supporting Information (Figure S2) and increase up to molar ratio 1.1 (in terms of polymer repeat units), after which they decrease. This reflects a decrease in the hydrodynamic size at lower molar ratios due to interaction of $C_{12}E_5$ with the polymer, through either peeling off from (multichain) clusters or solubilization of PBS-PFP monomers. While, as will be shown later, molecular dynamics calculations performed on two polymer chains and eight $C_{12}E_5$ monomers show that both of these are viable processes, we favor the peeling-off mechanism because the concentration of free PBS-PFP monomers in water is likely to be extremely small. As will be shown later, molecular dynamics calculations performed on two polymer chains and eight $C_{12}E_5$ monomers show that both of these are viable processes. Above the molar ratio 1.1, which under these conditions is around the cmc of $C_{12}E_5$, the polymer−surfactant complexes grow into more elongated structures from rods to supramolecular objects containing several complexes and D therefore decreases. At the highest molar ratio investigated (10.5), considerable errors may be present, such that only a part of the size distribution is detected ($qR_g \gg 1$), and a plateau is reached at low D values.

To shed more light on the structural change of the complexes, the amplitudes of the relaxation modes (A_{fast} and A_{slow} in eq 5) in the relaxation time distributions for different molar ratios were also analyzed. From the amplitudes, it is possible to calculate the scattering contribution of each mode to the overall scattering intensity using the following relation of the total static light scattering intensity (I), which is normalized to the incoming laser intensity:

$$I = I_{fast} + I_{slow} = [A_{fast}/(A_{fast} + A_{slow})]I + [A_{slow}/(A_{fast} + A_{slow})]I \quad (5)$$

In Figure 3, the scattering intensity of the slow translational mode and the fast mode are presented as a function of the molar ratio and the $C_{12}E_5$ concentration.

A drastic decrease in I_{slow} is observed, which can be explained by an increase of interactions between surfactant and the polyelectrolyte resulting from the breakup of polymer multichain clusters. At the same time, we note that the intensity of the fast relaxation process increases, which is compatible with the formation of more elongated structures for high $C_{12}E_5$/PBS-PFP molar ratio. I_{slow} follows the same trend as the total scattering intensity, which also decreases upon increasing molar ratio. Electrical conductivity measurements were made on aqueous solutions of the polymer in the presence of surfactant at the same $C_{12}E_5$/PBS-PFP molar ratio and polymer concentration, 1.2×10^{-4} M (in terms of repeat units), and are also presented in Figure 3. It can be seen that the three regimes, 1, 2, and 3, observed in our previous SANS study,[13d] can be distinguished in all three data sets. We feel that these correspond to small CPE clusters, mixed PBS-PFP/$C_{12}E_5$ micelles, and larger aggregates. Similar behavior has been observed by fluorescence measurements with the cationic CPE poly{9,9-bis[6-(*N*,*N*,*N*-trimethylammonium)hexyl]fluorene-*co*-1,4-phenylene} iodide in water in the presence of $C_{12}E_5$.[9a]

To obtain more experimental information on the structure of the mixed polymer−surfactant aggregates, binary $C_{12}E_5$/water and ternary $C_{12}E_5$/PBS-PFP/water samples with $C_{12}E_5$ concentration of 12.7 mM and $C_{12}E_5$/PBS-PFP molar ratio of 24.3 were investigated by SAXS. As worm- or threadlike micelles are expected in these two samples,[13d,13g,49−51] a cylindrical symmetry was assumed for data evaluation. Experimental SAXS intensities and corresponding IFT[29] fits are shown in Figure 4. Simply from inspection of these raw scattering curves, we can easily notice an increase in the forward scattering at very low q values upon introducing PBS-PFP polymer into the $C_{12}E_5$ micelles indicating a micellar growth. However, due to the limited resolution of the available q regime of the SAXS data, we must be cautious about commenting on the length of these micelles based on these data. We should note, in particular, that such an increase in the scattering intensity either could reflect the actual growth of the micelles or could equally only mean that the polymer makes the wormlike micelle less flexible, leading to longer "persistence" lengths of the aggregate seen in SAXS. We therefore restrict ourselves to obtaining information on the micellar cross section that is readily available within the accessible q regime.

This information is revealed through the cross-sectional $p_c(r)$ function shown in Figure 5a, which clearly indicates radially inhomogeneous scattering particles. The cross-sectional $p_c(r)$

(49) Brown, W.; Pu, Z.; Rymdén, R. *J. Phys. Chem.* **1988**, *92*, 6086–6094.
(50) Glatter, O.; Strey, R.; Schubert, K. V.; Kaler, E. W. *Ber. Bunsen-Ges.* **1996**, *100*, 323–335.
(51) Kato, T.; Anzai, S.; Seimiya, T. *J. Phys. Chem.* **1990**, *94*, 7255–7259.

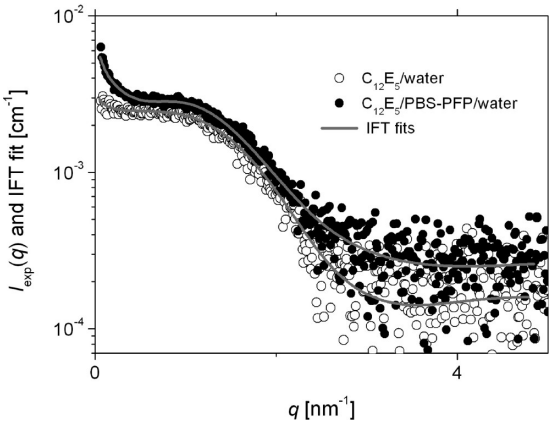

Figure 4. Experimental SAXS intensities on an absolute scale and the corresponding fits for the 12.75 mM $C_{12}E_5$ solution and mixed solution with 12.7 mM $C_{12}E_5$ and 0.52 mM (repeat unit) PBS-PFP (molar ratio 24.3).

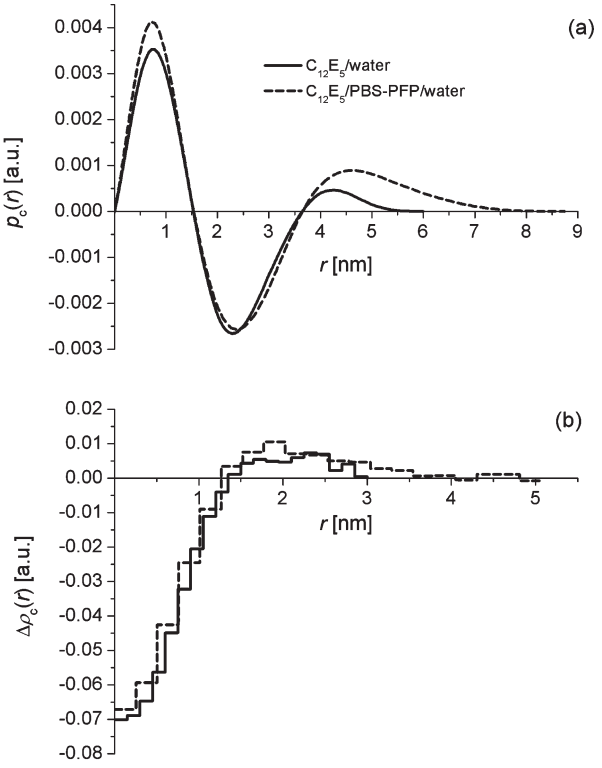

Figure 5. (a) Pair−distance distribution functions of the cross section $p_c(r)$ and (b) the corresponding electron density profile of the cross section $\Delta\rho_c(r)$ for 12.7 mM $C_{12}E_5$ solution and mixed solution with 12.7 mM $C_{12}E_5$ and 0.52 mM PBS-PFP (in terms of repeat units; molar ratio 24.3:1).

function can be further evaluated to yield the radial electron density profile of the micellar cross section $\Delta\rho_c(r)$ shown in Figure 5b. These results reveal the internal structure of the inhomogeneous scattering particles. Interestingly, the micellar core does not seem to be changed markedly (core radius of 1.3 nm) when PBS-PFP polymer is incorporated into the micelle, although the surfactant/polymer aggregate hydrophilic shell is somewhat increased (from the total radius, including the shell, of ca. 3 nm to ca. 4 nm).

All these experimental SAXS results on the micellar structure are in good agreement with the cryo-TEM imaging and simulation results discussed in the following sections and with the findings from other experimental methods. They also nicely correlate with the previous SANS findings on micellar cross sections from Knaapila et al. (see Figure 8 in ref 13d), although those measurements were carried out at a somewhat lower surfactant concentration.[13d]

The macroscopic translational diffusion coefficient D of a rodlike macromolecule obtained in the DLS studies may be expressed as a function of the length L of the rod and the axial ratio p ($= L/d$, where d is the diameter of the rod). Tirado et al.[52] have reformulated the modified Broersma expressions[53] that are applicable over a wide range of p values (see eqs S1, S2, and S3 in the Supporting Information). An effective (or apparent) diffusion coefficient of $(4.8 \pm 0.3) \times 10^{-12}$ m^2/s of the PBS-PFP-$C_{12}E_5$ aggregate was obtained in the DLS experiments on the filtered MR (mole ratio) 2.2 solution. According to the SANS investigation on the same system, the aggregate at this molar ratio was found to be rodlike.[13d] Using eqs S1, S2, and S3 in the Supporting Information together with the measured D value and taking the radius of the rod as equal to 4 nm (obtained from the SAXS measurements for the MR 24.3 sample, see Figure 5b), a rod length of 410 nm could be calculated (using the error in D, the range is 378−446 nm). In this calculation, we have assumed that the radius of the rod does not change when increasing the surfactant concentration. This value is considerably larger than that obtained in the SANS data analysis (80 ± 8 nm).[13d] However, in comparing these results, there are several assumptions of the rod models which need to be considered. Of particular importance is the fact that the different expressions existing for relating the diffusion coefficient of a rodlike macromolecule to its length are only thought to be valid for rigid, noninteracting rods (i.e., the infinite dilution case).[54] However, although, in these measurements, the diffusion coefficient was measured at a finite concentration for MR 2.2, and intermolecular interactions, therefore, are present; this cannot solely explain the large discrepancy between these two values. The difference is more likely to be due to the limited resolution of the q range of the small angle scattering measurements, which will lead to an underestimation of the length of rodlike macromolecules of this size. It is also important to note that the PBS-PFP-$C_{12}E_5$ mixed aggregates at MR 2.2 are polydisperse and are not completely rigid, and that both the flexibility and polydispersity may also contribute to the observed discrepancy in length.

Considering the behavior at high surfactant concentrations, where DLS suggests aggregate growth, cryo-TEM images in a related polymer-$C_{12}E_5$ system have shown that very large, rodlike objects were formed,[55] while TEM micrographs of dodecyl substituted poly(*p*-phenylene)sulfonates in water have also demonstrated large wormlike and looplike structures.[56] We have carried out cryo-TEM studies both of $C_{12}E_5$/PBS-PFP in water and of the surfactant alone in this concentration range. Figure 6A and B displays cryo-TEM images of a 19×10^{-3} M $C_{12}E_5$ solution, without added PBS-PFP, and it is evident that this sample contains a mixture of threadlike complex species of various length, as is expected at this concentration.[49−51,57] In Figure 6A, one can observe elongated threadlike structures having a maximum contour length of approximately 120 nm,

(52) Tirado, M. M.; Martínez, C. L.; de la Torre, J. G. *J. Chem. Phys.* **1984**, *81*, 2047–2052.
(53) Broersma, S. *J. Chem. Phys.* **1981**, *74*, 6989–6990.
(54) Schillén, K.; Brown, W.; Johnsen, R. M. *Macromolecules* **1994**, *27*, 4825–4832.
(55) Fütterer, T.; Hellweg, T.; Findenegg, G. H.; Frahn, J.; Schlüter, A. D.; Böttcher, C. *Langmuir* **2003**, *19*, 6537–6544.
(56) Kroeger, A.; Deimede, V.; Belack, J.; Lieberwirth, I.; Fytas, G.; Wegner, G. *Macromolecules* **2007**, *40*, 105–115.
(57) Bernheim-Groswasser, A.; Wachtel, E.; Talmon, Y. *Langmuir* **2000**, *16*, 4131–4140.

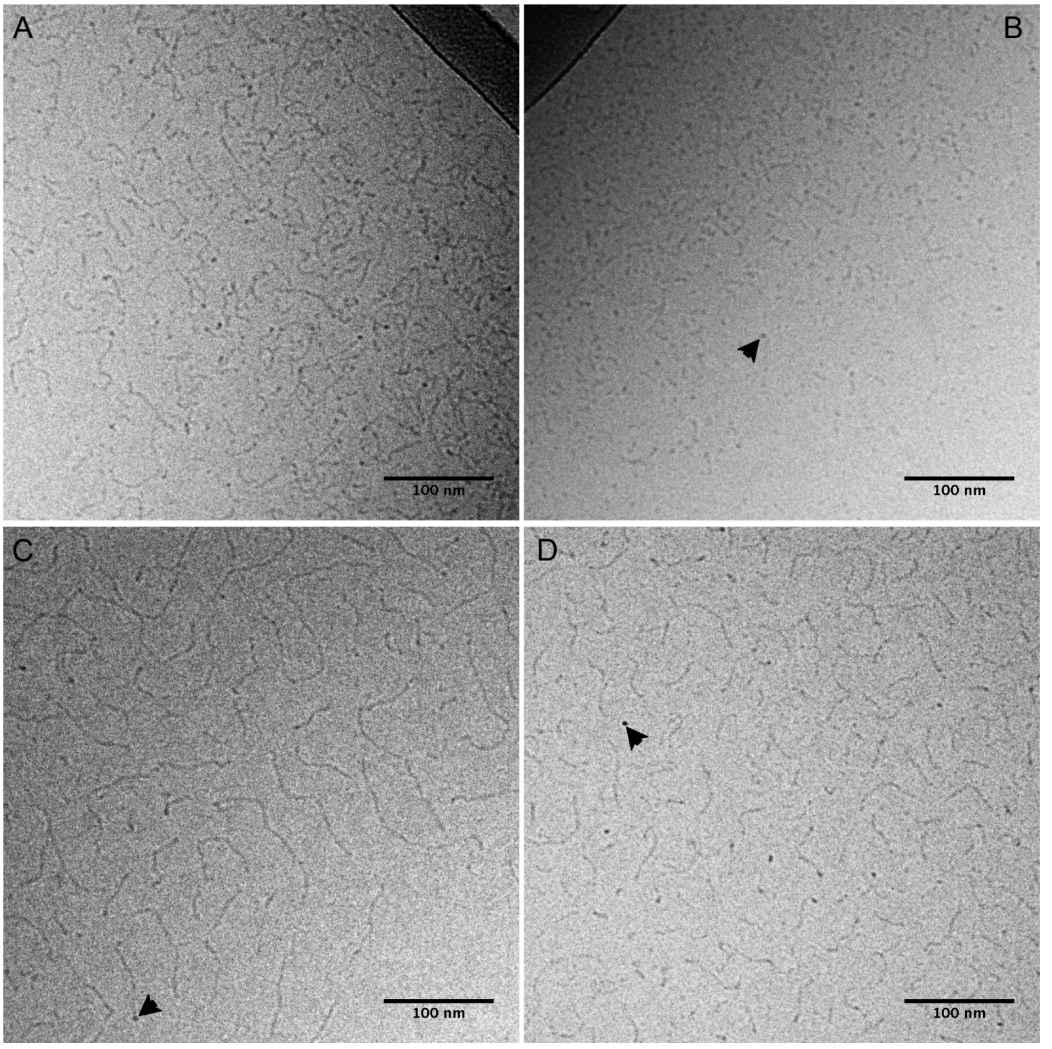

Figure 6. Cryo-TEM images of threadlike micellar aggregates of $C_{12}E_5$ alone (A, B) and in the presence of PBS-PFP (C, D), at a $C_{12}E_5$ concentration of 19×10^{-3} M. In the PBS-PFP containing sample (C, D), the $C_{12}E_5$/PBS-PFP molar ratio (in terms of repeat units) was kept at 8.8. Black arrowheads indicate high contrast spots, interpreted as being threadlike aggregates imaged along their long axis.

although most structures are significantly shorter (< 60 nm). Furthermore, the aggregates seem to be straight and very flexible. The round objects have much higher contrast than the threadlike structures (see arrowhead in Figure 6B) and are interpreted as short threadlike micellar aggregates imaged along their long axis. This result is in good agreement with those from the DLS study at the highest surfactant-to-polymer molar ratios.

For the PBS-PFP containing sample, we observe similar threadlike structures as in the pure $C_{12}E_5$ sample. However, the structures are significantly longer (< 280 nm) and, possibly, somewhat more rigid in the presence of the polymer (see Figure 6C and D). Furthermore, no difference is seen in the diameter of the aggregates irrespective of the presence of PBS-PFP. From the cryo-TEM images, a tentative diameter of between 3 and 4 nm is measurable and most probably represents the core. From the cryo-TEM analysis, it can be concluded that the presence of PBS-PFP results in growth of threadlike micelles, compared to the pure $C_{12}E_5$ sample. This can be explained by the incorporation of PBS-PFP within the micelles without any alteration of the diameter of the mixed polymer−surfactant aggregates. This is consistent with the SAXS data presented earlier as well as simulation results presented in the following section.

B. Molecular Dynamics Simulations on Aqueous PBS-PFP/$C_{12}E_5$ Systems. Molecular dynamics provides further details on the behavior of the system and on the nature of the mixed PBS-PFP/$C_{12}E_5$ micelles. As in our previous study,[13f] we have used a model based on a tetramer of PBS-PFP in the presence of water. Two different and distinct simulations (I and II) have been carried out, as summarized in Table 1. In the first case, we have studied the interaction between a PBS-PFP tetramer and four $C_{12}E_5$ molecules. This system attained a conformation very close to that of equilibrium in less than 2 ns of unrestrained dynamics. In the snapshot depicted in Figure 7, it is shown how closely the surfactant interacts with the polymer, forming a "core−shell" type structure with the rigid poly(1,4-phenylene-*alt*-fluorene) backbone, surrounded by the polymer side chains mixed with the surfactant to give a very hydrophilic exterior. Although the simulations are not intended to provide a detailed structure of the mixed PBS-PFP/$C_{12}E_5$ micelles, they strongly suggest that at least one surfactant molecule is necessary for each CPE repeat unit. Note also, in particular, that the anionic sulfonate groups are exposed to water. Further, it is apparent that the interaction between the surfactants and the fluorene backbone is not site specific.

In the second model system, the initial simulation box consists of two aggregated PBS-PFP tetramers, resulting from a previous equilibration in the absence of surfactant molecules, located in the center of the box. Eight molecules of $C_{12}E_5$ were then randomly placed around the polymer aggregate at distances

Table 1. Simulation Details for the Molecular Dynamics Calculations

	I	II
PBS-PFP tetramer	1	2
$C_{12}E_5$	4	8
water	4951	6081
Na^+	8	16
box volume	158 nm^3	198 nm^3
average box length	L = 5.4 nm	L = 5.8 nm
MD run time	5 ns	65 ns

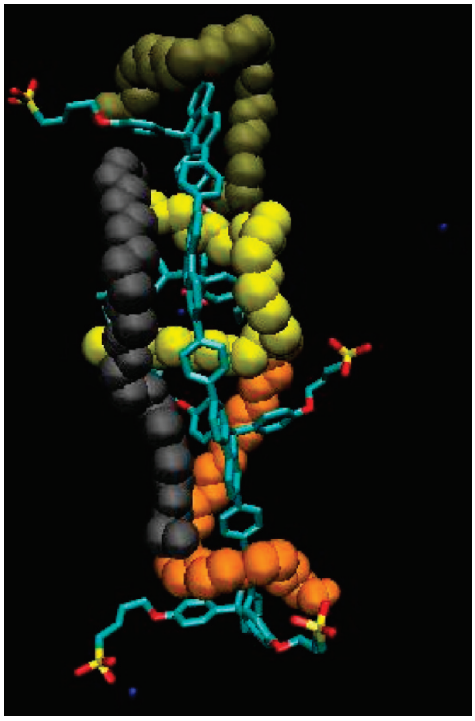

Figure 7. Molecular dynamics simulations of the interaction between a PBS-PFP tetramer and four $C_{12}E_5$ surfactants. The water molecules are not represented for clarity.

large enough so that the interaction with the polymer may be considered negligible (Figure 8a). Na^+ counterions were added to the system by randomly replacing solvent molecules (see Table 1).

The equilibration procedure, including restrained and unrestrained MD, prompted a close approach between surfactant and the aggregated polymers. The action of the surfactant upon this aggregate was assessed during the 65 ns production run (Figure 8b). It is observed that after 10 ns there is increasing separation between the polymer backbones, as demonstrated from the increase in the distance between the respective centers of mass (see Figure 9). A maximum distance of ca. 0.95 nm is reached after 40 ns, which remains approximately constant for the remaining part of the run.

Figure 8b presents the simulation box of the model system II after 65 ns, in which, for clarity, the water molecules are not represented. It can be seen that the tails of the surfactant intercalate between the two polymer backbones, inducing the separation of the latter. Due to computational cost, it was not possible to run this system for longer times. Nevertheless, the results clearly support the idea that the surfactant breaks up polyelectrolyte clusters and that, as mentioned for the previous model (I), with a single polymer tetramer and four $C_{12}E_5$ molecules, the surfactant molecules interact preferably with the polyfluorene backbone in a nonspecific way. The sulfonate groups are, again, exposed to the solvent.

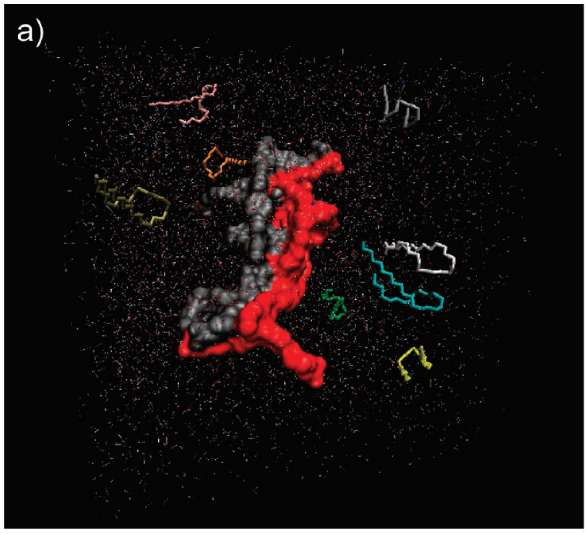

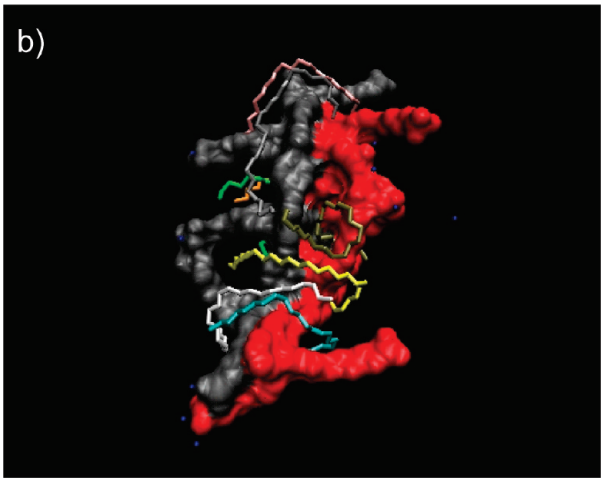

Figure 8. (a) Initial simulation box and (b) simulation box at 65 ns (water molecules are omitted for clarity).

C. Interaction of PBS-PFP with Other Nonionic Surfactants and Polymers. The effects of three other nonionic alkyloxyethylene surfactants on the absorption and emission spectra of PBS-PFP (6.8×10^{-3} g/L) in water have also been studied. In all cases, similar behavior was observed to that seen with $C_{12}E_5$ (Supporting Information Figure S1). Absorption spectra showed the typical broad band observed for polyfluorene derivatives, while, in all cases, a marked increase in fluorescence, accompanied by a blue shift on the structured fluorescence, was observed together with a narrowing of the spectra upon adding surfactant.

Fluorescence quantum yields were studied as a function of surfactant concentration for $C_{10}E_3$, $C_{12}E_4$, and $C_{12}E_5$ (Figure 10) and in all cases showed large increases in the region of the surfactant critical micelle concentration (using literature cmc values[58]). This strongly supports our previous suggestion that breakup of the polymer clusters is associated with micellization and incorporation of isolated chains of the polymer into polymer−surfactant aggregates. Spectral data and fluorescence quantum yields are given in Table 2. Data for Triton X-100 were only obtained for one concentration (above the cmc), since this is

(58) (a) Corkill, J. M.; Goodman, J. F.; Harrold, S. P. *Trans. Faraday Soc.* **1964**, *60*, 202–207. (b) Rosen, M. J.; Cohen, A. W.; Dahanayake, M.; Hua, X.-Y. *J. Phys. Chem.* **1982**, *86*, 541–545. (c) Huibers, P. D. T.; Lobanov, V. S.; Katritzky, A. R.; Shah, D. O.; Karelson, M. *Langmuir* **1996**, *12*, 1462–1470.

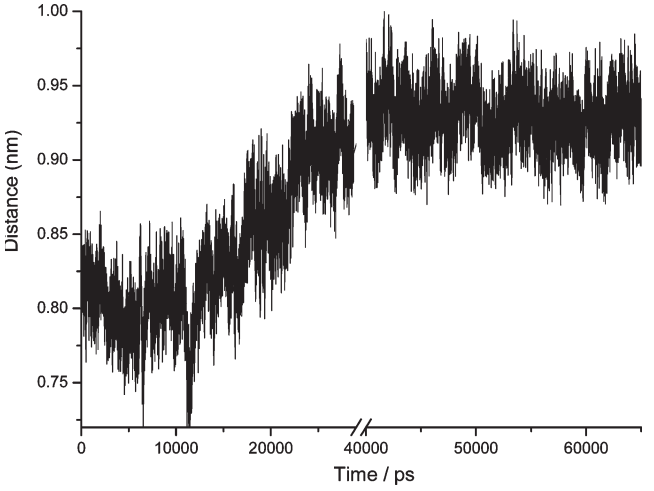

Figure 9. Distance between the centers of mass of the two oligomers.

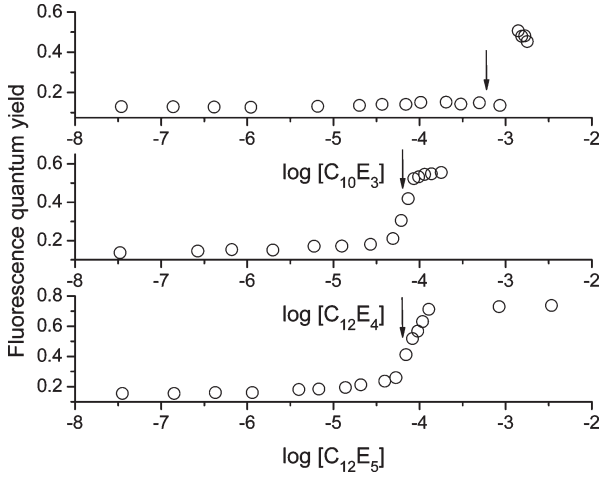

Figure 10. Fluorescence quantum yields for aqueous solutions of PBS-PFP (6.8×10^{-3} g/L, 9.18×10^{-6} (mole repeat units)/L) as functions of logarithm of concentrations of the nonionic surfactants $C_{10}E_3$, $C_{12}E_4$, and $C_{12}E_5$. Arrows show the critical micelle concentrations of the three surfactants.

a mixture of different chain length surfactants,[59] which limits quantitative interpretation of the behavior. It is noteworthy that the biggest fluorescence enhancement is observed with the two surfactants with the greatest number of oxyethylene units ($C_{12}E_5$ and Triton X-100). This may reflect the better ability of these longer sections to wrap round the 1,4-phenylene-fluorene backbone. Also, there are small, but significant, differences in the PBS-PFP fluorescence maximum with the four surfactants. A similar observation has been reported by Woo and co-workers for the fluorescence of a cationic fluorene−phenylene alternating copolymer in the presence of three nonionic surfactants.[9c] While we believe from the NMR and scattering experiments and the molecular dynamics simulations that the conjugated polyelectrolytes are dissolved at the molecular level in mixed polymer−surfactant aggregates in all these cases, these spectral shifts must represent some change in the local environment. As has been previously suggested for the solvatochromic properties of a series of polyfluorene derivatives,[60] this may well be associated with conformational changes of the relatively flexible polymer backbone. Precipitation has been reported with the cationic CPE poly {9,9-bis[6-(*N*,*N*,*N*-trimethylammonium)hexyl]fluorene-*co*-1,4-phenylene} iodide in water in the presence of Triton X-100.[9a] We did not observe this for the ternary system PBS-PFP/Triton X-100/water. However, alkyloxyethylene surfactants are known to phase separate (clouding) on heating.[18,61] As we have reported elsewhere,[18] these and other fluorene based conjugated polyelectrolytes increase the corresponding cloud points of the surfactants due to the formation of mixed aggregates (associative phase separation). It is worthy of note that the cloud points decrease upon adding salt, showing that the CPE−surfactant interactions involve a careful balance between hydrophobic and electrostatic interactions.

Table 2. Absorption (λ_{abs}) and Emission (λ_{em}) Spectral Maxima and Fluorescence Quantum Yields (Φ_f) of PBS-PFP (6.8×10^{-3} g/L, 9.18×10^{-6} (mole repeat units)/L) in Aqueous Solution without Surfactant and with Surfactant above the Critical Micelle Concentration

surfactant	λ_{abs} (nm)	λ_{em} (nm)	Φ_f
none	381	423	0.14
$C_{10}E_3$ (1.7×10^{-3} M)	368	413	0.48
$C_{12}E_4$ (3.8×10^{-3} M)	370	411	0.47
$C_{12}E_5$ (3.4×10^{-3} M)	370	410	0.74
Triton X-100[a]	371	410	0.72

[a] For the Triton X-100 data, the PBS-PFP concentration used was 2.84×10^{-3} g/L (3.83×10^{-6} (mole repeat units)/L).

The fluorescence spectra were recorded of aqueous solutions of PBS-PFP in the presence of various concentrations of poly (ethylene glycol) (PEG, molecular weights ($\overline{M}_n$) 200 and 10 000 g/mol). Similar behavior was seen with the two PEG polymers. Results for the high molecular weight derivative (10 000 g/mol) are given in Figure 11a. Over the concentration range studied, only small increases in the fluorescence intensity were seen with no significant shift in the emission band, indicating that PEG does not break up the PBS-PFP aggregates. This can be contrasted with the observations of strong interactions between PEG and an anionic poly(4,4′-diphenylene vinylene) (PDV) in aqueous solutions.[62] Although we do not have an explanation for the differences in behavior of PEG with PDV and with PBS-PFP, they may possibly be a consequence of the latter having hydrophobic groups in the two chains attached to the fluorene 9-position.

Also, in contrast to the behavior of PBS-PFP with PEG, with the end-capped hydrophobically modified poly(ethylene glycol) (HM-PEG, Figure 11b), both a blue shift in emission (to 418 nm) and a 19-fold increase in fluorescence quantum yield were seen, showing that, as was the case with the nonionic surfactants, the amphiphilic character of the polymer is a driving force for the breakup of aggregates.

Studies were also made of aqueous solutions of PBS-PFP in the presence of poly(propylene glycol) (PPG, $\overline{M}_n$ 425 g/mol). This is more hydrophobic than poly(ethylene glycol) and, as can be seen in Figure 11c, also leads to marked increases (5 times) in the fluorescence intensities, suggesting that it induces some breakup in the PBS-PFP polymer aggregates. There is also a smaller, but proportional, blue shift in the emission (ca. 1.5 nm). In contrast, the emission maxima in Figure 11a are identical in the absence and presence of PEG, which is compatible with the slight increase in the emission intensity in this case (about 1.7 times). While we do not, as yet, have a complete explanation for the phenomena seen with these water-soluble polymers, there appears to be a

(59) Hollis, G. L. *Surfactants Europa*; George Godwin: London, **1982; p 137.**
(60) Blondin, P.; Bouchard, J.; Beaupré, S.; Belletête, M.; Durocher, G.; Leclerc, M. *Macromolecules* **2000**, *33*, 5874–5879.
(61) Holmberg, K.; Jönsson, B.; Kronberg, B.; Lindman, B. *Surfactants and Polymers in Aqueous Solution*, 2nd ed.; John Wiley and Son: Chichester, **2003.**
(62) Wilson, J. S.; Frampton, M. J.; Michels, J. J.; Sardone, L.; Marletta, G.; Friend, R. H.; Samori, P.; Anderson, H. L.; Cacialli, F. *Adv. Mater.* **2005**, *17*, 2659–2663.

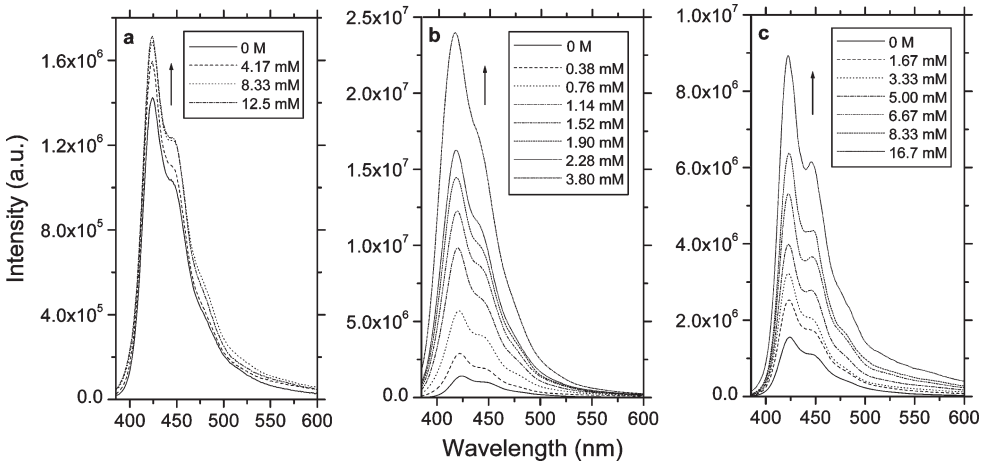

Figure 11. Fluorescence spectra of PBS-PFP (4.9×10^{-3} g/L) in aqueous solution (solid line) and in the presence of various concentrations of (a) PEG (molecular weight 10 000, 0−12.5 mM), (b) hydrophobically modified PEG (HM-PEG, 0−3.8 mM), and (c) poly(propylene glycol) (0−16.7 mM).

relationship between the increase in emission intensity and the extent of the blue shift, suggesting both have a common origin. In a study on solvent effects with a related cationic CPE, Wang and Bazan have strongly suggested that solvent effects on spectra and changes in aggregation state are not separable phenomena in this kind of system.[3f] Comparison of the blue shifts in PBS-PFP emission maxima and the small variations in the vibrational structure in the spectra with hydrophobically modified PEG and PPG seen in Figure 11b and c, and also observed in the presence of the nonionic surfactants, suggests that relatively small differences in structure of these nonionic systems can lead to significant changes in local environment, reflecting differences in their interactions with the CPE. As discussed in related studies on the interaction between this conjugated polyelectrolyte and gemini surfactants in aqueous solutions,[13f] we believe that a sensitive balance between hydrophobic and hydrophilic effects is involved in the interaction of cosolvents, surfactants, and water-soluble polymers with the conjugated polyelectrolyte PBS-PFP. In addition, since conformational changes of the relatively flexible fluorene-phenylene backbone[60] may be involved in the solvent effect on the emission maxima, the rigidity of the microenvironment in the region of the chromophore may also play a role.

Conclusions

Upon addition of nonionic surfactants to aqueous dispersions of the conjugated polyelectrolyte {1,4-phenylene-[9,9-bis(4-phenoxy-butylsulfonate)]fluorene-2,7-diyl} copolymer (PBS-PFP), marked blue shifts in the fluorescence spectra, increases in emission intensity, and changes in the vibronic structure of the emission spectrum are observed. The onset of interaction is seen to occur in the region of the surfactant critical micelle concentration and is interpreted as resulting from surfactant induced breakup of polymer clusters. More detailed studies were made for the system with $C_{12}E_5$, and dynamic and static light scattering studies confirmed earlier SANS measurements of the existence of three concentration regimes corresponding to the breakup of PBS-PFP clusters, formation of polymer−surfactant micellelike aggregates, and growth into supramolecular structures. The formation of mixed polymer−surfactant aggregates was confirmed by small-angle X-ray scattering results, which provided experimental insight into the internal structure of the inhomogeneous mixed surfactant−polymer aggregates. The breakup of polymer clusters leads also to an increase in the electrical conductivity of polymer in solution as is shown with $C_{12}E_5$ around its cmc. However, further additions of surfactant do not increase the electrical conductivity in solution, which agrees with the formation of elongated polymer−surfactant complexes with lower mobility. This is supported by cryo-TEM studies, which also suggest an increased stiffness in the polymer−surfactant aggregates as compared to the pure surfactant aggregates. The effect of interaction between the surfactant and conjugated polyelectrolyte is confirmed by MD simulations, which demonstrate the tendency to form polymer−surfactant aggregates in which isolated chains of PBS-PFP are included. Similar behavior is seen with hydrophobically modified poly(ethylene glycol) or with poly(propylene glycol). The changes are similar to those observed upon addition of organic cosolvents but occur at very much lower concentrations, suggesting the importance of binding of the surfactant or water-soluble polymer to the conjugated polyelectrolyte. In addition, the MD simulations show that the CPE backbone is surrounded in a sheath of surfactant molecules, while the sulfonate group is clearly exposed to water. This may have implications in the complexing of these anionic groups by oppositely charged species. For example, it is known that calcium(II) quenches anionic CPEs by inducing aggregation.[63] We have been interested in developing systems involving conjugated polyelectrolytes self-assembled with oppositely charged metal complexes for light harvesting, and have found with PBS-PFP and tris(bipyridyl) ruthenium(II) that $C_{12}E_5$ appears to inhibit aggregation of the CPE chains by this cationic metal complex.[64] This may be associated, at least in part, to the formation of a protective sheath of surfactant molecules around the CPE backbone. This behavior shows similarities to cyclodextrin-threaded conjugated systems which have been suggested to have potential as isolated molecular wires.[65]

Acknowledgment. We are indebted to Professor U. Olsson (Lund University) for the gift of highly pure nonionic surfactants. We thank a referee for stimulating comments on the importance of local environment on the emission spectra of this class of polymers. We are grateful to the FCT for the award of a post-doctoral fellowship (S.M.F., Grant SFRH/BPD/34703/2007) and

(63) Jiang, H.; Zhao, X.; Schanze, K. S. *Langmuir* **2006**, *22*, 5541–5543.
(64) Burrows, H. D.; Fonseca, S. M.; Dias, F. B.; Seixas de Melo, J.; Monkman, A. P.; Scherf, U.; Pradhan, S. *Adv. Mater.* **2009**, *21*, 1155–1159.
(65) Cacialli, F.; Wilson, J. S.; Michels, J. J.; Daniel, D.; Silva, C.; Friend, R. H.; Severin, N.; Samori, P.; Rabe, J. P.; O'Connell, M. J.; Taylor, P. N.; Anderson, H. L. *Nat Mater.* **2002**, *1*, 160–164.

a Ph.D. grant (C.L.S., Grant SFRH/BD/14213/2003). MEC and FEDER are thanked for financial support through the project MAT2004-03827, and POCI/FCT/FEDER through the project POCI/QUI/58291/2004. We thank the Linnaeus Center of Excellence on Organizing Molecular Matter (OMM) through the Swedish Research Council. We are grateful to the Slovenian Research Agency and GRICES for financial support for the collaboration between Ljubljana and Coimbra through the project BI-PT/4.1.1 Portugal-Slovenia 2008-2009 "Effect of the polymer hydrophobicity and backbone rigidity on polyelectrolyte−surfactant interactions", and to MEC/CRUP (*Acções Integradas*) for the collaboration between Burgos and Coimbra. Universidad de Burgos is also thanked for financial support of a short stay of M.J.T. in Coimbra University.

Supporting Information Available: Normalized absorption and emission spectra of PBS-PFP in aqueous solution alone and upon adding $C_{12}E_5$ (Figure S1). Apparent diffusion coefficient from DLS as a function of $C_{12}E_5$/PBS-PFP molar ratio at 298 K (Figure S2). Equations used in the determination of size from the DLS measurements. This material is available free of charge via the Internet at http://pubs.acs.org.